Heliyon 10 (2024) e34810

Contents lists available at ScienceDirect

Heliyon

journal homepage: www.cell.com/heliyon

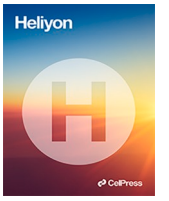

Research article

LncRNA ERICD interacts with TROAP to regulate TGF-β signaling in hepatocellular carcinoma

Yujie Xia [a], Bin Zhang [b], Nanrun Chen [c], Xiaowei Hu [a], Xinzhe Jin [a], Chenbin Lu [a], Feng Liang [a,*]

[a] *Department of Clinical Laboratory, Key Laboratory of Clinical Laboratory Diagnosis and Translational Research of Zhejiang Province, the First Affiliated Hospital of Wenzhou Medical University, Wenzhou, Zhejiang, China*
[b] *Qingdao Hospital, University of Health and Rehabilitation Sciences (Qingdao Municipal Hospital) , China*
[c] *Yongkang Municipal Center for Disease Control and Prevention, Zhejiang 321300, China*

A R T I C L E I N F O

Keywords:
Hepatocellular carcinoma
lncRNA ERICD
miR-142-5p
Invasion
Migration

A B S T R A C T

Hepatocellular carcinoma (HCC) is one of the most prevalent and common malignant tumors worldwide, accounting for 85–90 % of primary liver cancer cases. Accumulating evidence shows that long non-coding RNAs (LncRNAs) play regulatory roles in HCC occurrence and progression. However, little is known about the biological role of the LncRNA "E2F1-regulated inhibitor of cell death" (ERICD) in HCC. Our study revealed that ERICD is highly expressed in HCC and correlates with TNM staging; high ERICD levels were associated with poor patient prognoses. We revealed the targeting relationship between ERICD and miR-142-5p for the first time by bioinformatics prediction and further verified the targeting relationship between ERICD and miR-142-5p using a luciferase reporting experiment. In summary, our results showed that ERICD promotes the occurrence and metastasis of HCC by downregulating miR-142-5p expression. Our study provides a target for new potential therapeutic strategies for HCC.

1. Introduction

Hepatocellular carcinoma (HCC) is one of the most common gastrointestinal malignancies. According to the 2018 epidemiological statistics, the incidence and mortality rates of HCC ranked sixth and fourth worldwide [1,2]. Although substantial progress has been made in the treatment of HCC in recent years, such as the improvement of chemotherapy drugs and the continuous innovation of surgical methods, the overall prognosis of patients has not significantly improved. Most HCC patients have missed the optimal window for surgical treatment at the time of diagnosis, and the prognosis is very poor [3,4]. Even when surgical treatment is possible, the 5-year survival rate is poor due to frequent recurrence, metastasis, or the development of new primary lesions. The small-molecule targeted drug sorafenib demonstrates low clinical efficacy in HCC patients, and the development of drug resistance is common; thus, this treatment only prolongs the median patient survival time by 3 months [5,6]. Therefore, understanding the specific molecular biological mechanisms of HCC recurrence and metastasis is required to prevent such processes and improve HCC patient survival outcomes.

Long non-coding RNAs (LncRNAs) are non-coding transcripts over 200 base pairs in length generated by RNA polymerase II

* Corresponding author. Department of Clinical Laboratory, The First Affiliated Hospital of Wenzhou Medical University, (Nanbaixiang Site) Nanbaixiang, Ouhai district, Wenzhou, Zhejiang province, 325000, China.
E-mail address: liangfeng9076@163.com (F. Liang).

https://doi.org/10.1016/j.heliyon.2024.e34810
Received 20 February 2023; Received in revised form 15 July 2024; Accepted 17 July 2024
Available online 19 July 2024

transcription. LncRNAs interact with various molecules, including DNA, RNA, and proteins, and play a role in regulating cell processes such as gene transcription, mRNA translation, and intracellular protein localization and degradation [7,8]. The mechanisms by which LncRNAs regulate gene expression are complex. LncRNAs can directly affect gene expression by trapping or guiding chromatin modification and transcription mechanisms and affect mRNA splicing, nuclear–cytoplasmic shuttling, and translation [9,10]. LncRNAs can also regulate the expression of specific pathway proteins and post-translational modification [11,12]. Thus, there exists a regulatory network of specific cellular pathways mediated by LncRNAs. LncRNAs demonstrate regulated, tissue-specific expression across different tumors. LncRNAs related to various genomic functions affecting cell cycle, proliferation, immunity, and pluripotency can also be directly regulated by key oncogenes or tumor suppressor genes [13–15].

MicroRNAs (miRNAs) are small, non-coding single-stranded RNAs, approximately 22 nucleotides in length. Over 2500 mature miRNAs have been identified in the human genome. MiRNAs can negatively regulate gene expression by interfering with the translation or cleavage of mRNA targets [16,17]. MiRNAs are abnormally expressed in cancer and act as tumor suppressor genes or oncogenes during carcinogenesis. MiRNAs can alter biological processes by regulating target mRNAs [18,19]. For example, miRNAs have been found to function as oncogenes or tumor suppressor genes regulating tumor processes, including tumor cell genesis, proliferation, differentiation, invasion and metastasis, metabolism, and apoptosis [20,21]. The downregulation of miR-142-5p expression in pancreatic cancer, lung cancer, and other malignant tumor cells has been found to cause the overexpression of downstream pro-oncogenes, such as phosphatidylinositol-3-kinase, thereby promoting malignant cell proliferation [22–25].

TROAP is a cytoplasmic protein required for microtubule cytoskeleton regulation and spindle assembly [26]. Recent studies have found that TROAP plays an important role in various cancers. High TROAP expression is associated with poor cancer prognosis. Reducing the expression of this protein in tumor cells inhibits the proliferation and metastasis of tumor cells, indicating that TROAP is closely related to cell proliferation [27,28]. Li et al. confirmed that TROAP helps enhance the proliferation, invasion, and metastasis of breast cancer cells and may be an indicator of adverse prognoses in breast cancer [29]. Jing et al. found that TROAP mRNA was upregulated in gastric cancer tissues and associated with poor patient survival [30]. Bioinformatics analyses have revealed that TROAP is specifically expressed during liver regeneration and in HCC; however, there are few studies on the role of TROAP in liver cell proliferation and its underlying regulatory mechanisms.

At present, there are few studies on LncRNA ERICD in tumors, we focused on the role of the LncRNA "E2F1-regulated inhibitor of cell death" (ERICD) in HCC development. We verified the mechanism by which the LncRNA ERICD/miR-142-5p/TROAP axis plays a role in the degree of HCC malignancy using clinical samples, cells, and animals, providing a new theoretical basis for the prevention and treatment of HCC in clinical practice.

2. Materials and methods

2.1. Tissue specimens

HCC and adjacent (>5 cm from the tumor) tissues were collected from 15 HCC patients at the First Affiliated Hospital of Wenzhou Medical University. The Ethics Committee of the First Affiliated Hospital of Wenzhou Medical University (KY2022-R200) reviewed the collected samples. None of the 15 patients received preoperative targeted drug therapy or chemoradiotherapy. The patients provided informed consent for the use of their tissue samples, and the hospital Institutional Review Board approved the study. The collected samples were stored frozen in liquid nitrogen.

2.2. Cell lines and cell culture

The HCC cell lines HepG2 and Huh7 and the human embryonic renal epithelial cell line 293T were purchased from the Shanghai Cell Bank of the Chinese Academy of Science; the human normal liver epithelial cell line THLE-3 was purchased from American Type Culture Collection (ATCC, USA). The above cell lines were cultured in Dulbecco's Modified Eagle Medium (DMEM) containing 10 % fetal bovine serum (FBS) in an incubator at 37 °C with 5 % CO_2. All cell lines were confirmed to be mycoplasma free before the experiment and were identified using short tandem repeat (STR) analysis.

2.3. qRT-PCR

First, TRIzol was added to the collected cells or tissues; the samples were then mixed well, divided into aliquots, and placed on ice for 5 min. Two hundred microliters of chloroform was added to each sample. The samples were then vortexed for 10 s and incubated at room temperature for 5 min. After centrifugation at 12,000 rpm per minute for 20 min at 4 °C, 500 μL supernatant was transferred to a new centrifuge tube and 500 μL isopropanol was added. The tube was gently mixed by inverting and incubated for 10 min at room temperature. The tubes were then centrifuged for 15 min under the abovementioned conditions. The supernatant was discarded, and the pellet was washed with 75 % ethanol and resuspended in 20 μL DEPC-treated water. The RNA concentration was then determined using a NanoDrop 8000 spectrophotometer based on the intrinsic absorption properties of nucleic acids (DNA and RNA) at 260 nm. To obtain cDNA, 1 μg RNA was added to an RNAase-free centrifuge tube, gDNA Wiper Mix solution was added to remove genomic DNA, and 1 μL reverse transcription polymerase was added. The reverse-transcribed cDNA was used for quantitative PCR as per the SYBR Premix Ex Taq (Perfect Real-Time) quantitative kit directions. The total volume of the miR-142-5p PCR was 10 μL, including 1 μL cDNA template, 5 μL SYBR Green Mastermix, 1 μL each of the forword and reverse primers, and 2 μL double-distilled water. The reaction conditions were 95 °C for 15 s, 95 °C for 10 s, 60 °C for 40 s, and 70 °C for 10 s; 35 cycles were applied. The total volume of the TROAP

mRNA PCR was 20 μL, including 2 μL cDNA template, 1 μL each of the upstream and downstream primers, 10 μL SYBR Green Mastermix, and 6 μL double-distilled water. The reaction conditions were 95 °C for 1 min followed by 30 cycles of 95 °C for 20 s, 62 °C for 30 s, and 72 °C for 30 s. At the end of the amplification reaction, the melting curve was generated and the cycle threshold (CT) number was collected. Using U6 or GAPDH as an internal reference, the relative mRNA expression levels of miR-142-5p and TROAP were calculated using the $2^{-\Delta\Delta CT}$ method. Primers and their optimized annealing temperatures are listed in Table 1.

2.4. Dual-luciferase reporter gene assay

Luciferase activity analysis can sensitively detect the interaction of transcription factors with the promoter region of the target gene or miRNA with the 3′UTR of the target gene by measuring the biofluorescence released by luciferin oxidation by luciferase. LAR II, Stop & Glo Buffer, 50 × Stop & Glo Substrate, and 5 × PLB were equilibrated to room temperature (Promega, Madison, WI, USA). Deionized water was used to dilute 5 × PLB to 1 × PLB, and 50 × Stop & Glo Substrate was diluted to 1 × Stop & Glo Substrate in Stop & Glo Buffer. Cells were cultured in 24-well plates, and plasmids were transfected according to the Dual Luciferase Reporter Assay System (Promega). The cell culture medium was discarded, and the cells were washed with PBS twice. One hundred microliters of cell lysis buffer (1 × PLB) was added to each well in the 24-well plate, and the plate was shaken for 15 min to allow full cell lysis. Twenty microliters of cell lysate was transferred into a 96-well white-bottom plate (E&K Scientific EK-25075), and 100 μL of the LAR II substrate was added to each well, and the fluorescence value (A) was measured using a multi-function measuring instrument (Molecular Devices). Then, 100 μL Stop & Glo buffer was added to the original reaction well to stop the LAR II luminescence reaction, and the fluorescence value (B) was determined. The ratio of A/B was used as the final relative fluorescence value.

2.5. Transwell invasion and migration assays

Cells in each group were transfected for 48 h and resuspended in serum-free medium, and the cell suspension density was adjusted to 1×10^5/mL. Two hundred microliters of cell suspension was added to the upper Transwell chamber, and 500 μL of DMEM containing 20 % FBS was added to the 24-well plate. The Transwell chamber was then incubated in a cell incubator at 37 °C with 5 % CO_2 and saturated humidity. After 16 h of culture, the Transwell chamber was removed, and the cells remaining in the upper chamber were gently swabbed. The cells were fixed with 4 % paraformaldehyde for 30 min, stained with 0.5 % crystal violet for 15 min, and photographed under an inverted phase contrast microscope. Five 400 × fields of view were randomly selected, and the number of cells penetrating the membrane was counted. The number of penetrating cells represented cell invasion ability. In the invasion experiment, matrix glue was added to the Transwell chamber. Cell images were recorded using a ZEISS microscope.

2.6. MTT assay

Cells with good growth status were seeded into 6-well plates, and transfection experiments were conducted at approximately 60 % confluency. At 48 h after transfection, the cells were digested with 0.25 % trypsin and transferred to 96-well plates at a density of 1×10^3 cells per well. After 0, 24, 48, and 72 h of incubation, 20 μL of 5 mg/mL MTT solution was added to each well, and the plates were incubated at 37 °C for 2 h. The supernatant was removed and discarded, 200 μL of DMSO was added, and the mixture was gently shaken to completely dissolve the crystals. The optical density (OD) of each well at 450 nm was measured using a microplate reader. The OD450 value represented cell proliferation activity.

2.7. Cell transfection

pcDNA3.1, PCDNA3.1-TROAP, miR-142-5p mimics NC, and miR-142-5p mimics were purchased from Shanghai Fuhui Biotechnology Co., LTD. Exponentially growing cells were seeded at 2×10^5 per well in 6-well plates and allowed to grow overnight at 37 °C in complete medium to 75 % confluency. The medium was removed after 24 h, and cells were washed three times with PBS. Lipofectamine 2000 was used for transient transfection of cells with the corresponding vector according to the manufacturer's directions and incubated in the corresponding medium at 37 °C with 5 % CO_2. All cells were maintained in the medium for at least 24 h before

Table 1
Primer sequences.

Genes		Sequence(5′-3′)	Annealling temperature(°C)
TROAP	Forward	TGCAGAAACCACCGCTCAATA	57
	Reverse	CCACCAATCTTTGTGATGTCTCT	55
ERICD	Forward	TTTCCCAGATTTCCCGGAGC	57
	Reverse	TTCGGAGGAAGTGCTGGTTC	57
miR-142-5p	Forward	CAUAAAGUAGAAAGCACUACU	48
	Reverse	UAGUGCUUUCUACUUUAUGUU	47
U6	Forward	AGTAGTGCTTTCUACTTTACG	50
	Reverse	CAGCACCCCCGAGTAGTACAA	58
GAPDH	Forward	ACCCACTCCTCCACCTTTGAC	58
	Reverse	TGTTGCTGTAGCCAAATTCGTT	56

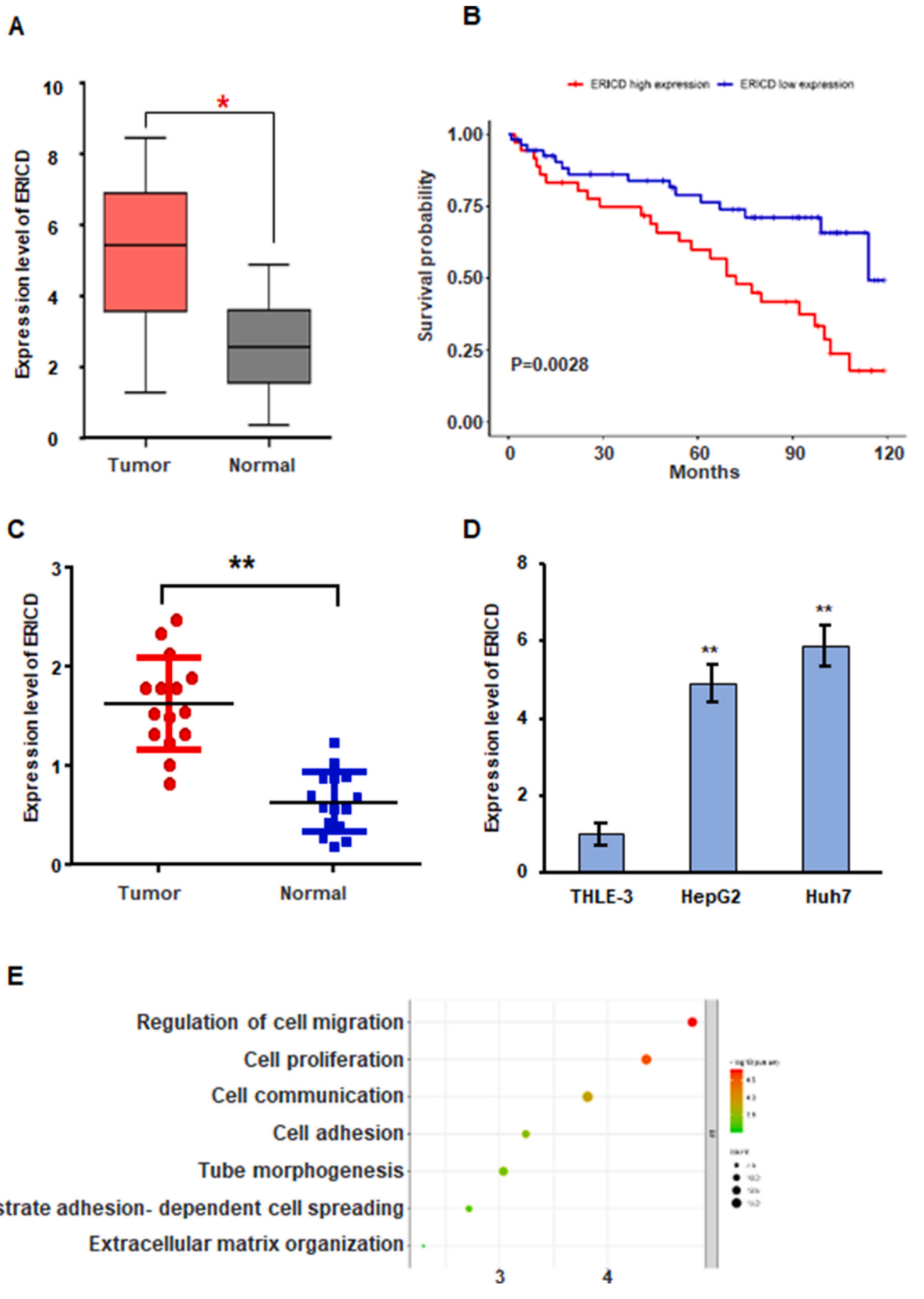

(caption on next page)

Fig. 1. LncRNA ERICD is highly expressed in HCC. (A) Expression of LncRNA ERICD in normal tissues and HCC tissues in The Cancer Genome Atlas database. (B) Kaplan–Meier survival analysis of HCC patients with positive or negative LncRNA ERICD expression. (C) Analysis of LncRNA ERICD expression in 15 HCC tissues and adjacent paired normal liver tissue samples. (D) qRT–PCR was used to measure the expression of LncRNA ERICD in normal liver and HCC cells. (E) KEGG analysis of the involved cellular processes. The data are presented as the mean ± S.D. *$P < 0.05$, **$P < 0.01$.

subsequent experiments.

2.8. EdU assay

Cells in the logarithmic growth phase were evenly inoculated in 24-well plates and cultured in an incubator at a constant temperature for 24 h so that the cell confluence reached 60 %. Then, 200 μL of 50 nM EdU working solution was added to each well and incubated for 2 h in an incubator at a constant temperature. The medium was then discarded, and the cells were washed two times with PBS buffer. Then, 4 % paraformaldehyde was added to fix the cells for 30 min, after which the fixative was discarded. Next, 2 mg/mL glycine solution was added to neutralize formaldehyde, and the cells were washed with PBS buffer. Under dark conditions, 200 μL Apollo staining reaction solution (Ruibo, Guangzhou) was added to each well, followed by incubation at room temperature for 30 min. An osmotic agent (PBS containing 0.5 % TritonX 100) was added to permeate the cells, followed by the addition of 1 × Hoechst33342 reaction solution and further incubation for 30 min. Cell images were recorded using a ZEISS confocal microscope.

2.9. Western blotting

RIPA lysis buffer containing PMSF was added to the collected tissues and cells, and lysis was conducted for 10 min on ice to extract total cell protein. Protein quantification was conducted using the BCA method, 5 × SDS loading buffer was added, and the protein was fully denatured in a metal bath at 95 °C for 10 min. The denatured protein (50 μg) was separated by SDS-PAGE (80 V followed by 120 V). After electrophoresis, the separated proteins were transferred to a PVDF membrane (constant flow of 250 mA for 90 min). The membranes were blocked with 5 % BSA for 2 h at room temperature. Primary antibodies were then added, and the membranes were incubated overnight at 4 °C. The next day, sheep anti-rabbit secondary antibody marked with biotin was added and the membranes were incubated for 1 h at room temperature. ECL luminescent reagents were added to the membranes, darkroom exposure was conducted, the film was developed, and ChemiScope 3300 mini software was used to analyze the images. GAPDH was used as the reference, and the ratio of the gray value of the electrophoretic band of the target protein to the gray value of the reference protein was to determine the relative expression level of the target protein. The primary antibodies were as follows:anti-TGF-β2(19999–1-P, Proteintech), anti-SMAD2/3(#8685, Cell Signaling Technology), anti-phospho SMAD3 (#9520, Cell Signaling Technology), and anti-GAPDH (#2118, Cell Signaling Technology).

2.10. Animal studies

The stable overexpressing LncRNA ERICD Huh7 cell lines in the logarithmic growth phase were resuspended in PBS, the cell density was adjusted to 3×10^7 cells/mL, and then they were rapidly injected into BALB/c nude mice (male, 4–6 weeks old, n = 3 mice in each group, SLAC Laboratory Animal Center) subcutaneously in the right dorsal side near the axilla. Tumor formation was monitored every two to three days using an intravital imaging system. Nude mice were euthanized four weeks after injection. The tumors were dissected and weighed. Maximum length (L) and minimum length (W) of the tumor were measured with a Vernier caliper, and the tumor volume was calculated as $V = L \times W2 \times 0.5326$. All animal experimental procedures were approved by the Animal Ethics Committee of the First Affiliated Hospital of Wenzhou Medical University.

2.11. Statistical analysis

The experimental data were calculated using GraphPadPrism version 6.0 (GraphPad Software, Inc.). Data were expressed as the mean ± standard deviation (mean ± SD), and differences between groups were analyzed using an unpaired *t*-test or one-way ANOVA followed by a Tukey test. $P < 0.05$ was considered statistically significant.

3. RESULTS

3.1. LncRNA ERICD expression is elevated in HCC

We first analyzed LncRNA ERICD expression by bioinformatics methods to explore its role in the occurrence and development of HCC. We found that LncRNA ERICD expression levels were significantly increased in patients with HCC, and prognosis worsened as LncRNA ERICD levels increased (Fig. 1A and B). We also analyzed the collected HCC samples and found that the expression level of LncRNA ERICD in HCC tissues was significantly higher than that in adjacent tissues (Fig. 1C). To further verify our inference, we measured the expression of LncRNA ERICD in normal hepatocytes and HCC cell lines. The qRT–PCR results showed that LncRNA ERICD expression levels in HCC cell lines were increased compared with those in normal hepatocytes (Fig. 1D). We performed a cluster analysis on LncRNA ERICD co-expressed genes to predict the gene function of LncRNA ERICD. Enrichment analysis was performed

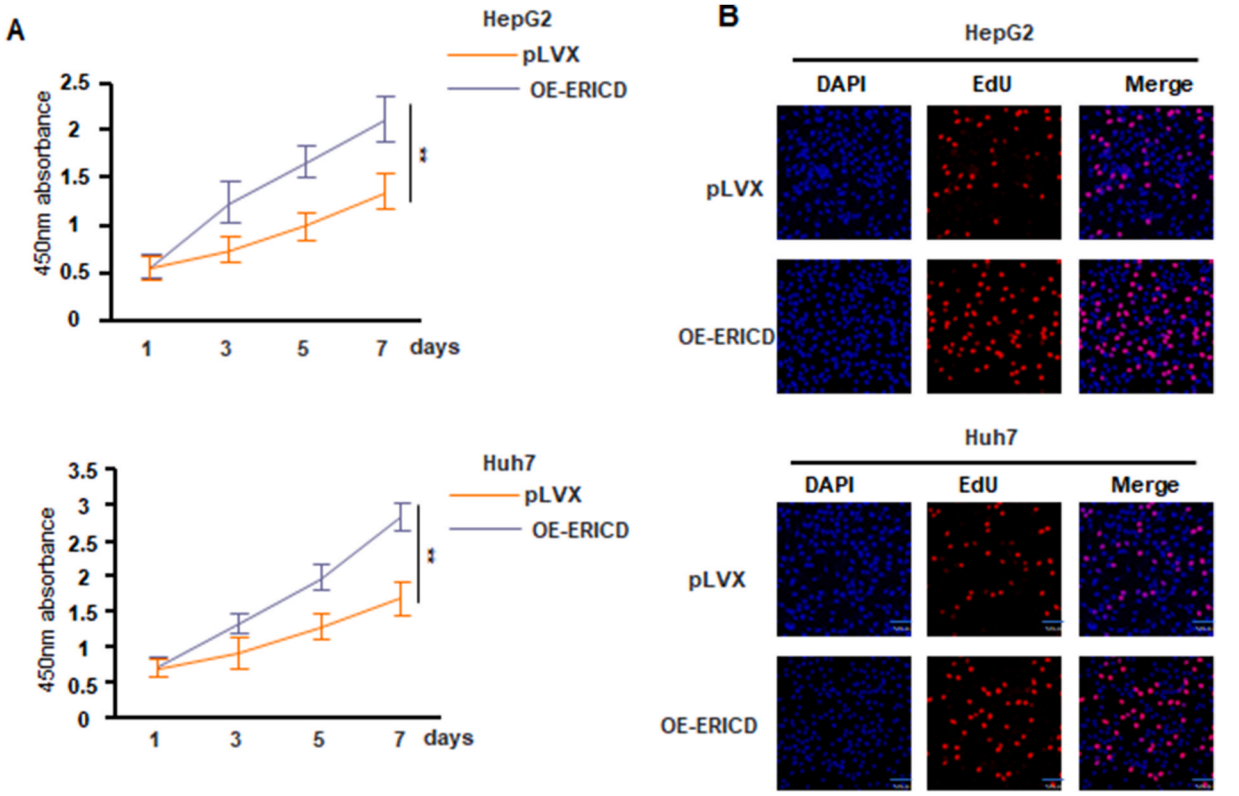

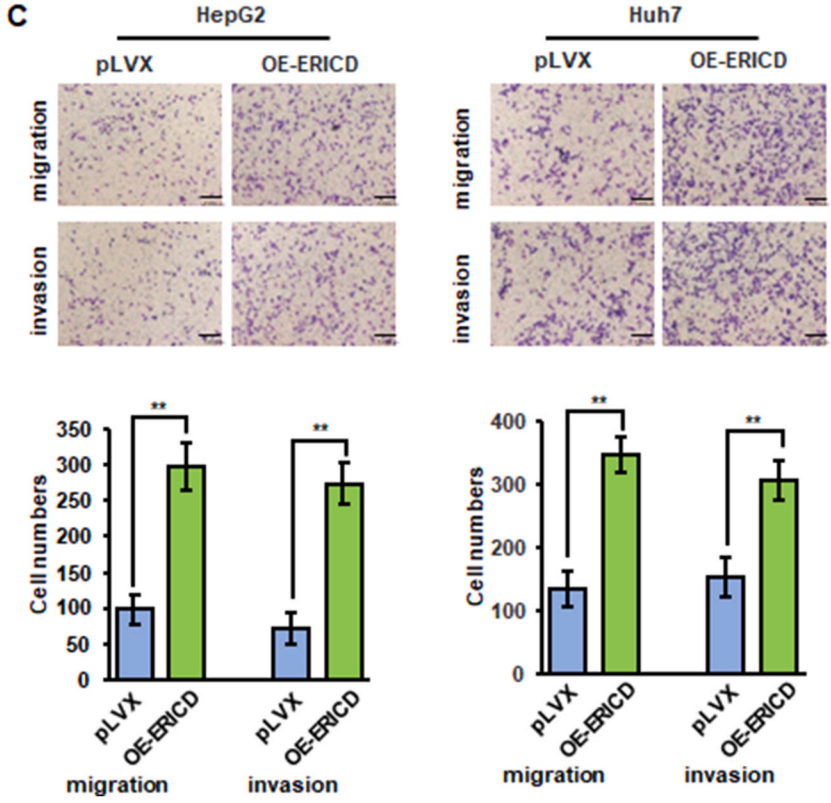

(caption on next page)

Fig. 2. LncRNA ERICD promotes the proliferation, migration, and invasion of HCC. The LncRNA ERICD overexpression plasmid plvx-ERICD or blank plasmid plvx-Con was transfected into HepG2 and Huh7 cells. (A, B) Cell proliferation was detected with MTT (A) and EdU (B) assays. (C) A Transwell assay was used to detect cell migration and invasion abilities. The data are presented as the mean ± S.D. *$P < 0.05$, **$P < 0.01$.

using the Database for Annotation, Visualization and Integrated Discover (DAVID) online analysis tool. The Kyoto Encyclopedia of Genes and Genomes (KEGG) analysis showed that LncRNA ERICD co-expressed genes were mainly involved in cell proliferation, migration, and invasion signaling pathways (Fig. 1E). All these results indicate that LncRNA ERICD promotes the occurrence and development of HCC.

3.2. LncRNA ERICD promotes the proliferation, migration, and invasion of HCC

Next, we overexpressed LncRNA ERICD plasmids in hepatocellular carcinoma cell lines HepG2 and Huh7, and MTT and EdU assay results showed that LncRNA ERICD promoted the proliferation of hepatocellular carcinoma cells (Fig. 2A and B). The Transwell assay results also showed that the migration and invasion abilities of HCC cell lines were significantly increased after LncRNA ERICD plasmid transfection (Fig. 2C). We also constructed a Huh7 cell line stably overexpressing LncRNA ERICD and injected the stably transformed cell line subcutaneously into immunodeficient mice. After 28 days, the mice were sacrificed, and the tumors were dissected and measured. We found that cells overexpressing LncRNA ERICD demonstrated significantly elevated tumor-forming capacities compared with control cells (Fig. 3A–C). Our experimental data indicate that LncRNA ERICD can promote the occurrence and development of

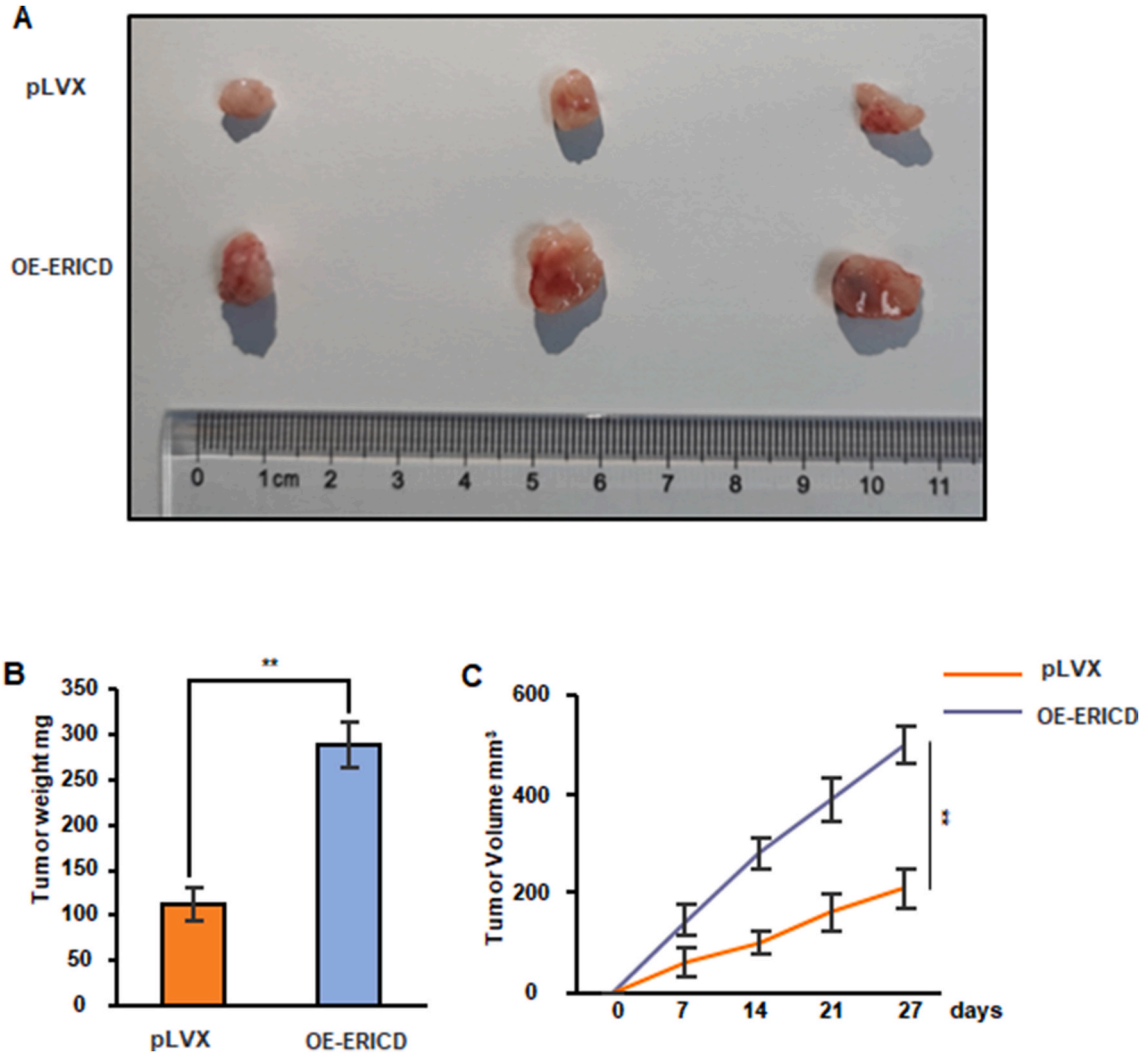

Fig. 3. LncRNA ERICD promotes HCC growth *in vivo*. Subcutaneous xenografts of Huh7 cells infected with ERICD overexpressing lentivirus or control lentivirus. (A) Images of the tumors from nude mice at necropsy are presented. (B, C) The average weight (B) and volume (C) of xenografted tumors were measured. Data are presented as the mean ± SEM. **$P < 0.01$.

HCC.

3.3. LncRNA ERICD sponge adsorbed miR-142-5p

To further elucidate the regulatory mechanism of LncRNA ERICD in HCC, we used TarBase v.8 and predicted that LncRNA ERICD could bind miR-142-5p (Fig. 4A). We further determined that LncRNA ERICD could bind miR-142-5p by a dual-luciferase assay (Fig. 4B). Furthermore, we measured the expression of miR-142-5p in normal hepatocytes and HCC cell lines and found that miR-142-5p expression was significantly downregulated in HCC cell lines compared with that in normal hepatocytes (Fig. 4C). Fluorescence *in situ* hybridization (FISH) experiments demonstrated that LncRNA ERICD and miR-142-5p co-localized in the cytoplasm of HCC cells

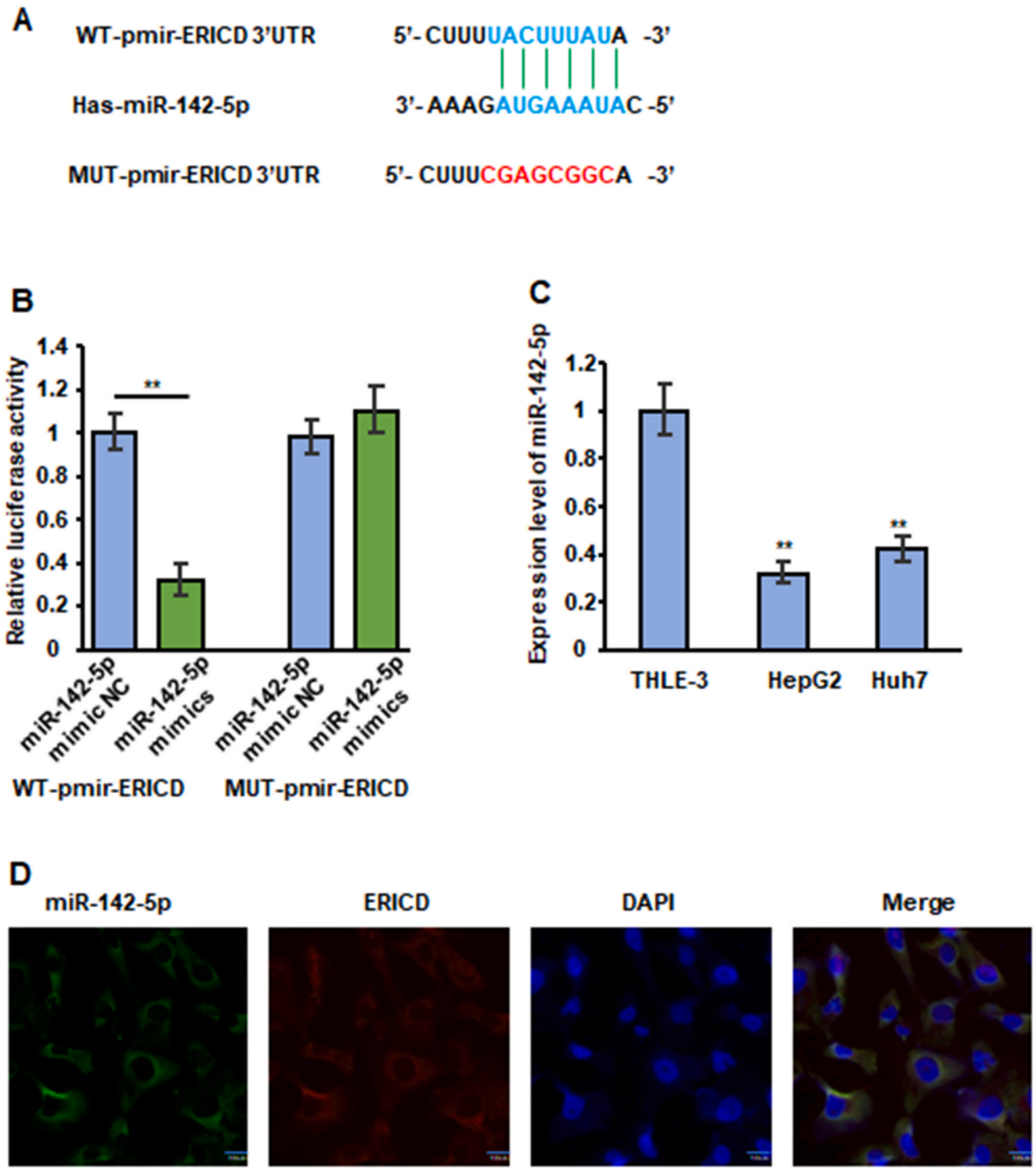

Fig. 4. LncRNA ERICD sponge adsorbed miR-142-5p. (A) The binding and mutation sites of LncRNA ERICD and miR-142-5p. (B) After transfection of LncRNA ERICD with miR-142-5p WT and MUT luciferase reporter genes, the luciferase activity in the cells was detected by a microplate reader. (C) qRT–PCR was used to measure the expression of miR-142-5p in normal liver and HCC cells. (D) FISH was used to verify the co-localization of LncRNA ERICD and miR-142-5p. Data are presented as the mean ± SEM. $^{**}P < 0.01$.

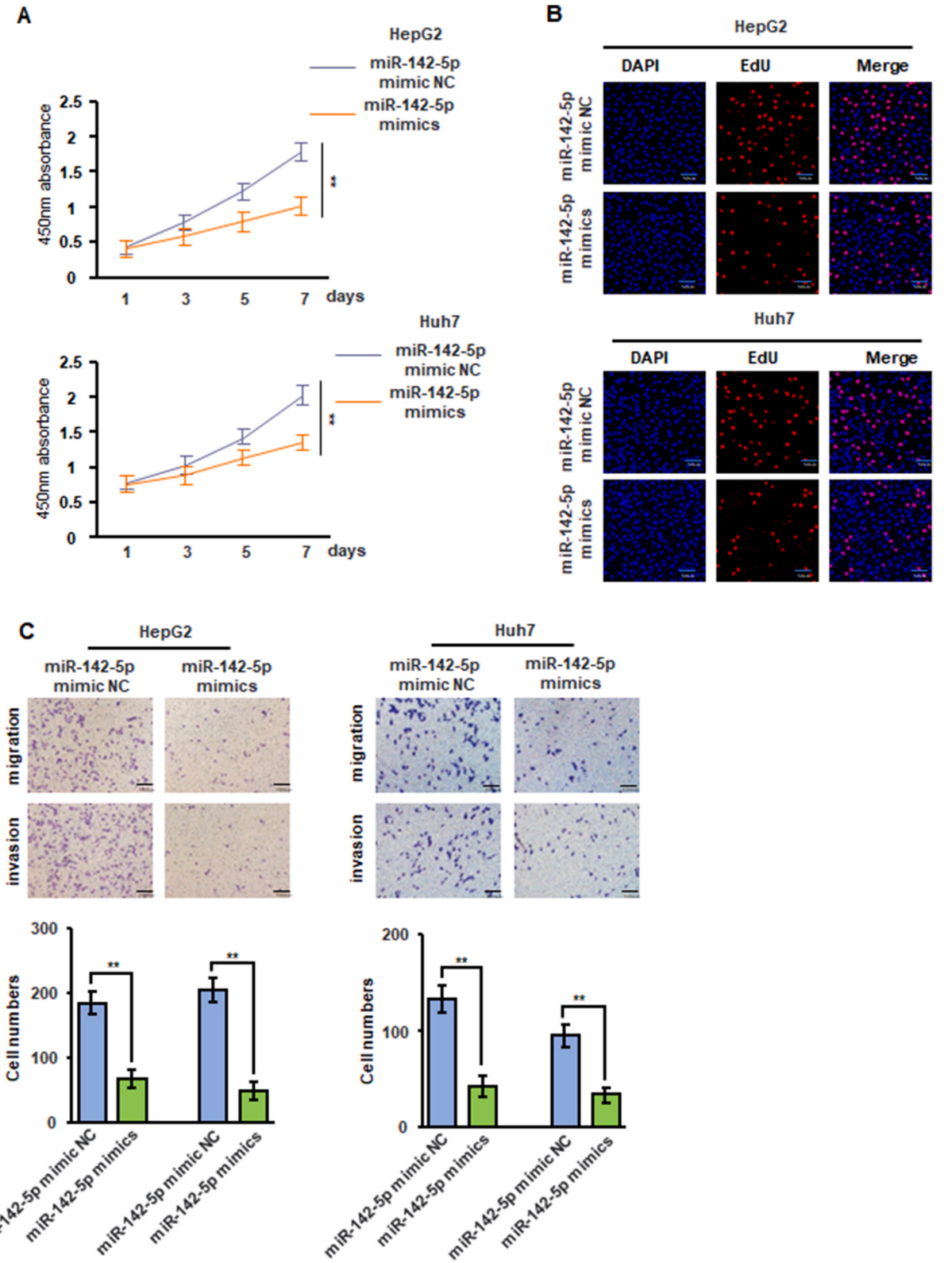

Fig. 5. miR-142-5p inhibits proliferation, migration, and invasion of HCC cells. HepG2 and Huh7 cells were transduced with the miR-142-5p mimic NC or miR-142-5p mimics. (A, B) Cell proliferation was detected with MTT (A) and EdU (B) assays. (C) A Transwell assay was used to detect cell migration and invasion abilities. The data are presented as the mean ± S.D. *$P < 0.05$, **$P < 0.01$.

(Fig. 4D). We transfected miR-142-5p mimics into hepatocellular carcinoma cell lines and found that the proliferation, migration, and invasion capacities of the cells were significantly reduced after the transfection of miR-142-5p mimics compared with those of the blank group (Fig. 5A–C).

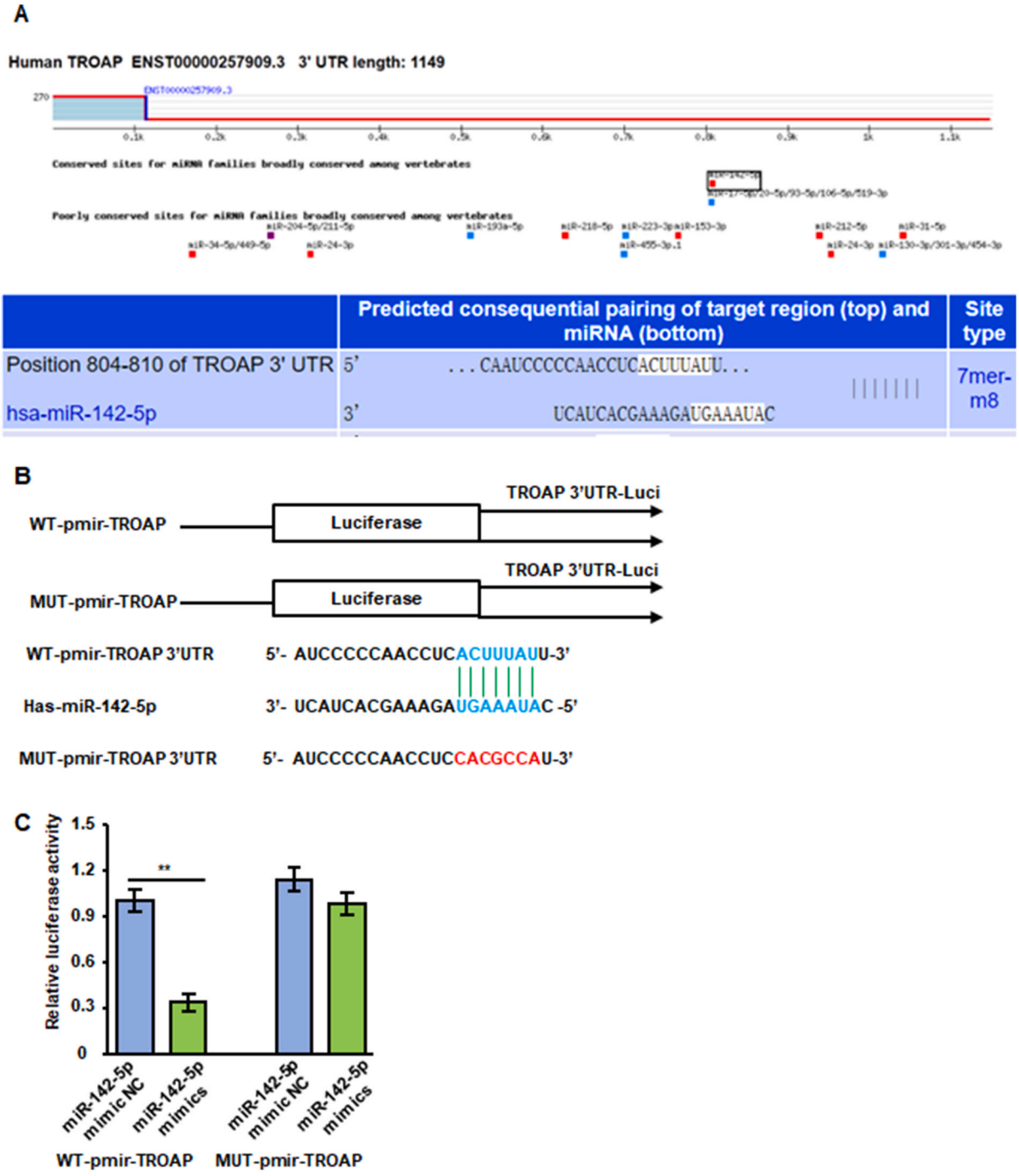

Fig. 6. miR-142-5p directly binds to the TROAP 3′-UTR. (A) The potential binding sites of miR-142-5p and TROAP were predicted using the TargetScan website. (B) The binding and mutation sites of miR-142-5p and TROAP 3′UTR. (C) After transfection of miR-142-5p and TROAP 3′UTR WT and MUT luciferase reporter genes, the luciferase activity in the cells was detected by a microplate reader. The data are presented as the mean ± S.D. *$P < 0.05$, **$P < 0.01$.

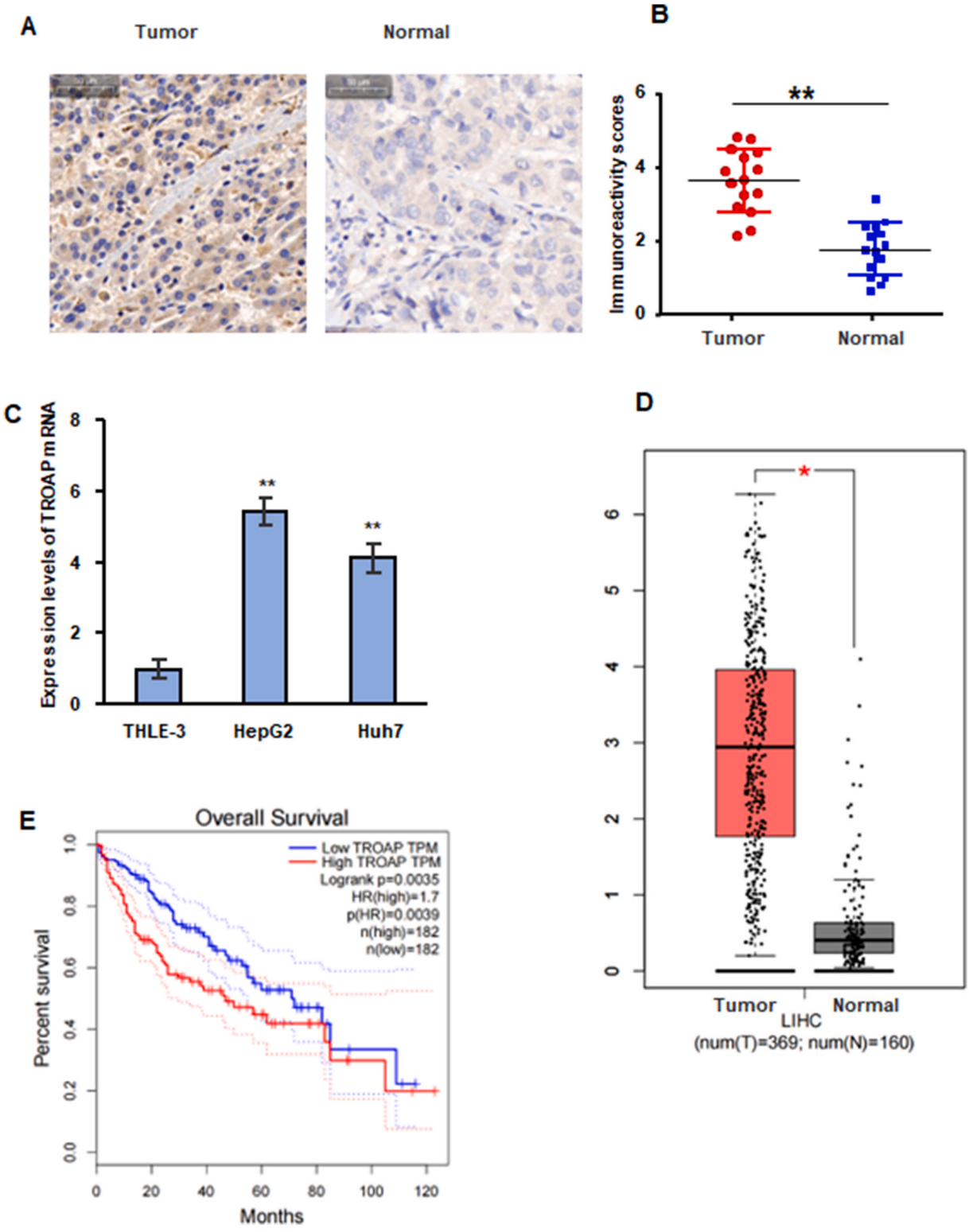

Fig. 7. TROAP is highly expressed in HCC. (A, B) Analysis of TROAP expression in 15 HCC tissues and adjacent paired normal liver tissue samples. (C) qRT–PCR was used to measure the mRNA expression of TROAP in normal liver and HCC cells. (D) Expression of TROAP in normal and HCC tissues from the TCGA database. (E) Kaplan–Meier survival analysis of HCC patients with positive or negative TROAP expression. The data are presented as the mean ± S.D. *$P < 0.05$, **$P < 0.01$.

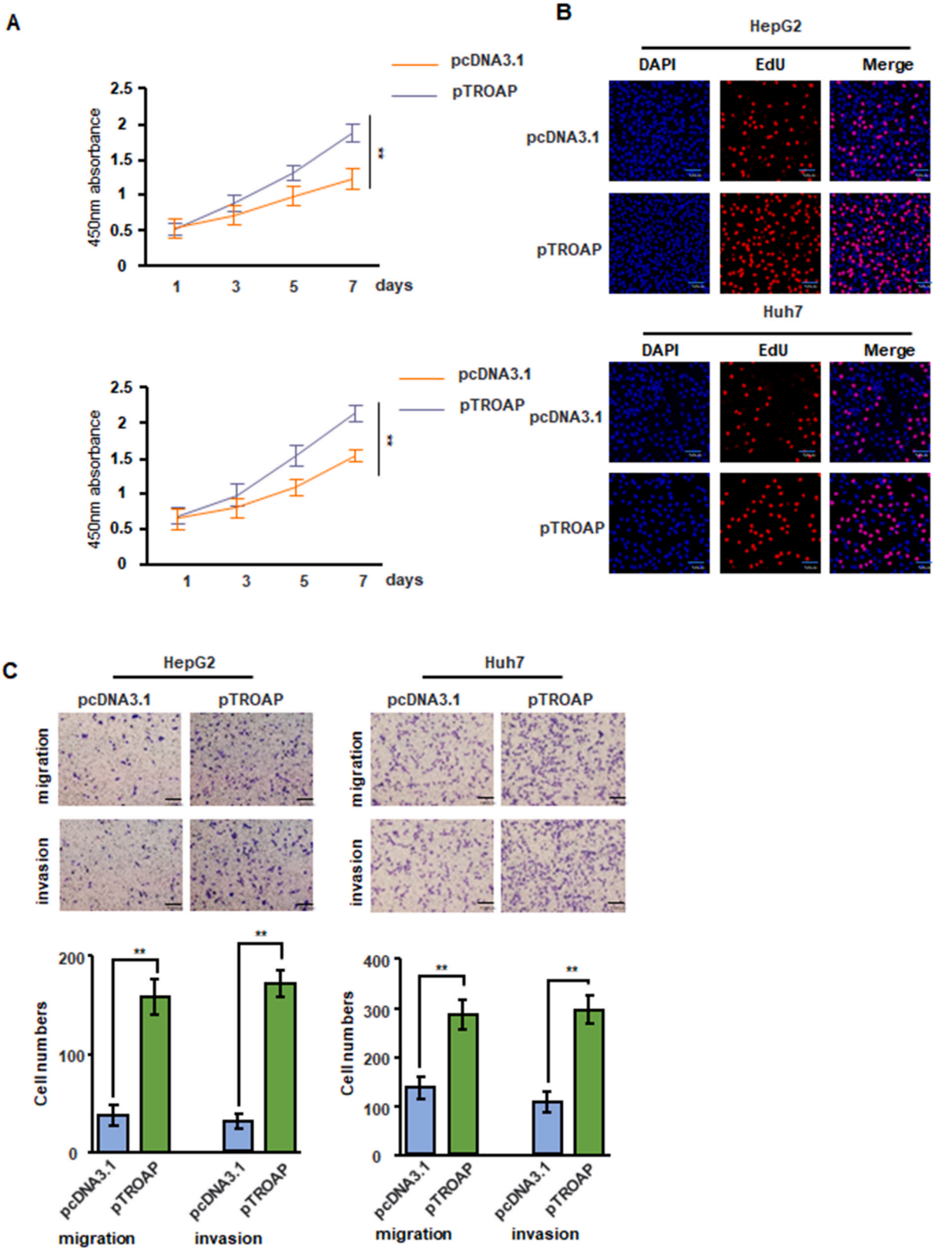

(caption on next page)

Fig. 8. TROAP promotes the proliferation, migration, and invasion of HCC. The TROAP overexpression pTROAP plasmid or blank pcDNA3.1 was transfected into HepG2 and Huh7 cells. (A, B) Cell proliferation was detected with MTT (A) and EdU (B) assays. (C) A Transwell assay was used to detect cell migration and invasion abilities. The data are presented as the mean ± S.D. *$P < 0.05$, **$P < 0.01$.

3.4. miR-142-5p directly binds to the TROAP 3′-UTR

TROAP was identified as a potential downstream target of miR-142-5p by TargetScan analysis (Fig. 6A). The potential binding sites of miR-142-5p and TROAP were predicted using the TargetScan website (Fig. 6B). The luciferase reporter gene assay showed that miR-142-5p significantly decreased the luciferase activity of TROAP 3′UTR-WT but had no effect on that of TROAP 3′UTR-MUT (Fig. 6C). We also conducted immunohistochemical analysis and scoring of HCC tissues, and the scoring results showed that TROAP expression was significantly upregulated in HCC tissues (Fig. 7A and B). TROAP expression was also significantly upregulated in hepatocellular carcinoma cells compared with that in normal hepatocytes (Fig. 7C). Bioinformatics analyses confirmed that TROAP expression was significantly increased in HCC patient samples, and patients with high TROAP expression had a poor prognosis (Fig. 7D and E). The proliferation, migration, and invasion abilities of HCC cells transfected with a TROAP overexpression plasmid were also significantly increased (Fig. 8A–C).

3.5. LncRNA ERICD regulates the TGF β pathway through the miR-142-5p/TROAP axis

Through the enrichment of the TROAP signaling pathway, we found that TROAP could regulate the TGF β pathway (Fig. 9A). The expression of TGF β2 was significantly increased when TROAP was overexpressed in HCC cell lines, (Fig. 9B). The western blotting results also showed that TGF β and downstream SMAD3 phosphorylation levels were significantly increased (Fig. 9C).

4. Discussion

Primary HCC is responsible for ~200,000 deaths annually worldwide. Each year, ~500,000 people are diagnosed with hepatic cancer, of which HCC accounts for over 90 %. HCC is the most common type of primary liver cancer. HCC patient survival depends on the disease severity [31]. Lobectomy can be performed for early HCC, and postoperative interventional chemotherapy, microwave ablation, and other local treatments can be used to prevent local recurrence and distant metastasis. If advanced HCC is not promptly controlled, the treatment efficiency and patient survival times are seriously diminished. Tumor invasion, metastatic dissemination, recurrence, and drug resistance have been identified as major causes of poor clinical outcomes in HCC patients [32]. Therefore, it is urgent to find new therapeutic targets for HCC.

In recent years, LncRNAs have become a focus of cancer-related research. There is considerable evidence that LncRNAs regulate cancer cell migration, proliferation, and apoptosis. In addition, miRNAs are increasingly found to be associated with various tumor processes, including tumor initiation, progression, and metastasis. Next-generation sequencing is a breakthrough technology that has redefined the landscape of human molecular genetic testing [10]. Bioinformatics is a novel interdisciplinary approach that develops and utilizes modern computational tools to analyze and interpret high-dimensional biological data. Next-generation sequencing technologies have revealed many disease-related genetic changes, and bioinformatics has become an important component of clinical disease research [33]. We found that LncRNA ERICD, upregulated in HCC, is closely associated with clinical survival prognosis. We first transfected ERICD overexpression plasmids into HCC cell lines HepG2 and Huh7 and found that overexpression of ERICD was followed by the downregulation of miR-142-5p and upregulation of TROAP. RNA was extracted from 15 HCC tissue samples, and our analysis revealed that ERICD and TROAP were highly expressed and positively correlated in HCC tissues. We verified the regulatory effect of ERICD on miR-142-5p and TROAP by transfecting plasmids overexpressing ERICD into HepG2 and Huh7 cells. Moreover, miR-144-5p was found to negatively regulate TROAP by transfection with a miR-142-5p mimic.

TROAP is necessary for spindle assembly regulation and centrosome integrity. TROAP was initially found to be closely related to embryo implantation, and the cellular process of embryo implantation is similar to malignant cell metastasis and invasion. Therefore, tumor cell invasion may share some molecular mechanisms with trophoblast invasion of maternal uterine tissue [26]. Recently, TROAP has been found to be involved in the proliferation, invasion, and migration of various cancers. However, there are few reports of TROAP in HCC and almost no literature related to its role in hepatocyte proliferation [34]. Therefore, we investigated the mechanism by which TROAP promotes cell proliferation in the liver. In this study, TROAP was overexpressed in HepG2 and Huh7 cells, and the effect of TROAP overexpression on the proliferation of these cells and the underlying mechanisms were investigated.

In summary, we explored the role and mechanism of LncRNA ERICD in regulating the invasion and migration abilities of HCC cells, providing new ideas and targets for HCC therapy.The disadvantage is that our clinical cases are too few, and we have not conducted a large number of clinical patient validation.

Funding

This work was financially supported by the Wenzhou Municipal Science and Technology Bureau of China (Y20220743) and Key Laboratory of Clinical Laboratory Diagnosis and Translational Research of Zhejiang Province (2022E10022).

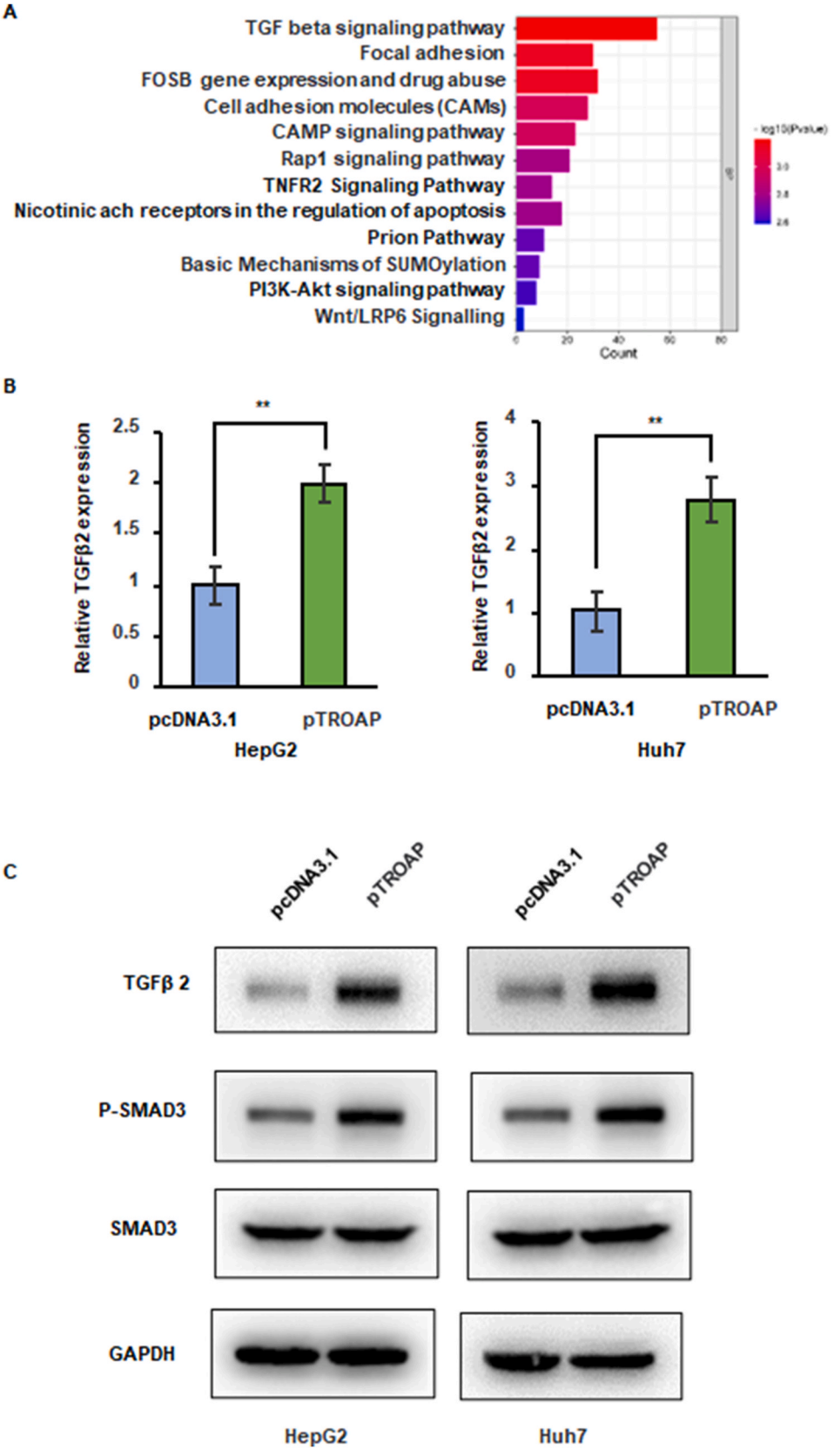

(caption on next page)

Fig. 9. LncRNA ERICD regulates the TGF β pathway through the miR-142-5p/TROAP axis (A) KEGG pathway analysis. The TROAP overexpression pTROAP plasmid or blank pcDNA3.1 was transfected into HepG2 and Huh7 cells. (B) qRT–PCR was used to measure the mRNA expression levels of TGF β. (C) Effects of miR-874-3p on protein levels of TGF β and phosphorylated SMAD3. The data are presented as the mean ± S.D. *$P < 0.05$, **$P < 0.01$.

Ethics approval and consent to participate

Our study complied with the Declaration of Helsinki and was approved by the hospital ethical review board (the First Affiliated Hospital of Wenzhou Medical University, Wenzhou, China, KY2022-R200). The informed written consent was obtained from all patients. All animal experimental procedures were approved by the Animal Ethics Committee of the First Affiliated Hospital of Wenzhou Medical University.

Availability of data and materials

All data will be shared upon reasonable request to the corresponding author. The datasets used and/or analyzed during the currentstudy are available from the corresponding author on reasonable request.

CRediT authorship contribution statement

Yujie Xia: Data curation, Conceptualization. **Bin Zhang:** Investigation, Data curation. **Nanrun Chen:** Project administration, Methodology, Data curation. **Xiaowei Hu:** Software, Methodology. **Xinzhe Jin:** Data curation. **Chenbin Lu:** Data curation. **Feng Liang:** Writing – review & editing, Writing – original draft, Funding acquisition, Formal analysis, Data curation, Conceptualization.

Declaration of competing interest

The authors declare that they have no known competing financial interests or personal relationships that could have appeared to influence the work reported in this paper.

Acknowledgements

We thank LetPub (www.letpub.com) for its linguistic assistance during the preparation of this manuscript.

Abbrevations

UTR	untranslated region
HCC	Hepatocellular carcinoma
LncRNAs	long non-coding RNAs

Appendix A. Supplementary data

Supplementary data to this article can be found online at https://doi.org/10.1016/j.heliyon.2024.e34810.

References

[1] Hepatocellular carcinoma, Nat. Rev. Dis. Prim. 7 (1) (2021) 7.
[2] N.D. Parikh, A. Pillai, Recent advances in hepatocellular carcinoma treatment, Clin. Gastroenterol. Hepatol. 19 (10) (2021) 2020–2024.
[3] M. Vyas, X. Zhang, Hepatocellular carcinoma: role of pathology in the era of precision medicine, Clin. Liver Dis. 24 (4) (2020) 591–610.
[4] N. Wen, et al., The clinical management of hepatocellular carcinoma worldwide: a concise review and comparison of current guidelines: 2022 update, Biosci Trends 16 (1) (2022) 20–30.
[5] E. Degasperi, M. Colombo, Distinctive features of hepatocellular carcinoma in non-alcoholic fatty liver disease, Lancet Gastroenterol Hepatol 1 (2) (2016) 156–164.
[6] C. Fountzilas, et al., Immunotherapy in hepatocellular cancer, Adv. Cancer Res. 149 (2021) 295–320.
[7] J. Zhu, et al., Function of lncRNAs and approaches to lncRNA-protein interactions, Sci. China Life Sci. 56 (10) (2013) 876–885.
[8] W. Lin, et al., LncRNAs regulate metabolism in cancer, Int. J. Biol. Sci. 16 (7) (2020) 1194–1206.
[9] H.M. Okuyan, M.A. Begen, LncRNAs in osteoarthritis, Clin. Chim. Acta 532 (2022) 145–163.
[10] M.C. Bridges, A.C. Daulagala, A. Kourtidis, LNCcation: lncRNA localization and function, J. Cell Biol. 220 (2) (2021).
[11] J. Liu, et al., Long noncoding RNA AGPG regulates PFKFB3-mediated tumor glycolytic reprogramming, Nat. Commun. 11 (1) (2020) 1507.
[12] L.J. Sang, et al., LncRNA CamK-A regulates Ca(2+)-signaling-mediated tumor microenvironment remodeling, Mol. Cell 72 (3) (2018) 601.
[13] P. Grote, R.A. Boon, LncRNAs coming of age, Circ. Res. 123 (5) (2018) 535–537.
[14] E.G. Park, et al., Tumor immune microenvironment lncRNAs, Briefings Bioinf. 23 (1) (2022).
[15] F. Kopp, J.T. Mendell, Functional classification and experimental dissection of long noncoding RNAs, Cell 172 (3) (2018) 393–407.
[16] T.X. Lu, M.E. Rothenberg, MicroRNA, J. Allergy Clin. Immunol. 141 (4) (2018) 1202–1207.

[17] M. Pilon, The copper microRNAs, New Phytol. 213 (3) (2017) 1030–1035.
[18] N. Bushati, S.M. Cohen, microRNA functions, Annu. Rev. Cell Dev. Biol. 23 (2007) 175–205.
[19] C. Schulte, M. Karakas, T. Zeller, microRNAs in cardiovascular disease - clinical application, Clin. Chem. Lab. Med. 55 (5) (2017) 687–704.
[20] Y.S. Lee, A. Dutta, MicroRNAs in cancer, Annu. Rev. Pathol. 4 (2009) 199–227.
[21] J. Hayes, P.P. Peruzzi, S. Lawler, MicroRNAs in cancer: biomarkers, functions and therapy, Trends Mol. Med. 20 (8) (2014) 460–469.
[22] R. Yao, et al., miR-142-5p regulates pancreatic cancer cell proliferation and apoptosis by regulation of RAP1A, Pathol. Res. Pract. 215 (6) (2019) 152416.
[23] X. Tang, et al., Regulating COX10-AS1/miR-142-5p/PAICS axis inhibits the proliferation of non-small cell lung cancer, Bioengineered 12 (1) (2021) 4643–4653.
[24] C. Zhou, et al., Exosome-derived miR-142-5p remodels lymphatic vessels and induces Ido to promote immune privilege in the tumour microenvironment, Cell Death Differ. 28 (2) (2021) 715–729.
[25] J. Zhang, et al., A novel homeostatic loop of sorcin drives paclitaxel-resistance and malignant progression via Smad4/ZEB1/miR-142-5p in human ovarian cancer, Oncogene 40 (30) (2021) 4906–4918.
[26] L. Li, et al., TROAP switches DYRK1 activity to drive hepatocellular carcinoma progression, Cell Death Dis. 12 (1) (2021) 125.
[27] X. Ye, H. Lv, MicroRNA-519d-3p inhibits cell proliferation and migration by targeting TROAP in colorectal cancer, Biomed. Pharmacother. 105 (2018) 879–886.
[28] H. Liu, et al., ASPM and TROAP gene expression as potential malignant tumor markers, Ann. Transl. Med. 10 (10) (2022) 586.
[29] K. Li, et al., TROAP promotes breast cancer proliferation and metastasis, BioMed Res. Int. 2019 (2019) 6140951.
[30] K. Jing, Q. Mao, P. Ma, Decreased expression of TROAP suppresses cellular proliferation, migration and invasion in gastric cancer, Mol. Med. Rep. 18 (3) (2018) 3020–3026.
[31] W. Wang, C. Wei, Advances in the early diagnosis of hepatocellular carcinoma, Genes Dis 7 (3) (2020) 308–319.
[32] S. Deng, A. Solinas, D.F. Calvisi, Cabozantinib for HCC treatment, from clinical back to experimental models, Front. Oncol. 11 (2021) 756672.
[33] T. Ali, P. Grote, Beyond the RNA-dependent function of LncRNA genes, Elife 9 (2020).
[34] H. Hu, et al., The upregulation of trophinin-associated protein (TROAP) predicts a poor prognosis in hepatocellular carcinoma, J. Cancer 10 (4) (2019) 957–967.